Finite Elements in Analysis and Design 46 (2010) 685–697

Contents lists available at ScienceDirect

Finite Elements in Analysis and Design

journal homepage: www.elsevier.com/locate/finel

Mechanical filtering characteristics of passive periodic engine mount

Woojin Jung [a], Zheng Gu [b], A. Baz [b,*]

[a] Agency of Defence Development, P.O. Box 18, Jinhae, Gyeongnam 645-600, South Korea
[b] Department of Mechanical Engineering, University of Maryland, College Park, MD 20742, USA

ARTICLE INFO

Article history:
Received 6 April 2009
Accepted 14 March 2010
Available online 10 April 2010

Keywords:
Periodic engine mount
Finite element analysis
Transfer matrix approach
Experimental validation

ABSTRACT

The transmission of automotive engine vibrations to the chassis is isolated using a new class of mounts which rely in their operation on optimally designed and periodically distributed viscoelastic inserts. The proposed mount acts as a mechanical filter for impeding the propagation of vibration within specific frequency bands called the "stop bands". The spectral width of these bands is enhanced by making the viscoelastic inserts operate in a shear mode rather than compression mode. The theory governing the operation of this class of periodic mounts is presented using the theory of finite elements combined with the transfer matrix approach. The predictions of the performance of the mount are validated against the predictions of the commercial finite element code ANSYS and against experimental results obtained from prototypes of plain and periodic mounts. The obtained results demonstrate the feasibility of the shear mode periodic mount as another means for blocking the transmission of vibration over a broad frequency band. Extending the effective width of the operating frequency bands of this class of mount through active control means is the ultimate goal of this study.

1. Introduction

A periodic structure consists of an assembly of identical elements connected in a repeated manner [1]. Examples of these structures can be found in many engineering applications such as satellite solar panels, wings and fuselages of aircraft, petroleum pipe-lines, railway tracks, submarines and many others.

In these structures, waves can propagate in some frequency bands called "pass bands" and are attenuated in others called "stop bands" [2–7]. Excellent reviews on the state-of-the-art have been given by Mead [7] and by Mester and Benaroya [8], where extended lists of references can be found. Since then, studies of the characteristics of periodic structures and their applications in engineering have been extensively investigated including passive and active periodic structures [9–17].

In this paper, the emphasis is placed on the development of a shear mode passive periodic engine mounts in order to effectively isolate the transmission of vibration from the engine to the chassis. This class of mounts is radically different from other conventional types of engine mounts such as the passive rubber mounts [18] and hydraulic engine mount [19,20] which are generally effective at narrow frequency ranges. It is equally as effective as other types of active engine mounts [21,22] which can operate over broader frequency ranges but at the expense of the classical complexity and reliability.

The effectiveness of the presented periodic engine mount stems from its unique design that relies in its operation on optimally designed and periodically distributed viscoelastic inserts in order to generate broad band filtering characteristics. Such characteristics enable the mount to completely block the propagation of the vibration rather than attenuating it. The spectral width of the operating band is enhanced by making the viscoelastic inserts operate in a shear mode rather than compression mode used in the passive periodic mount of Asiri [23].

The paper is accordingly organized in five sections. In Section 1, a brief introduction is given. In Section 2, a mathematical model of the shear mode periodic mount is presented and the equations of motion are derived from the finite element approach and then the transfer matrix is obtained. The basic filtering characteristics of these mounts are outlined in Section 3. Section 4 demonstrates the experimental results and numerical analysis using ANSYS. Section 5 summarizes the obtained results and conclusions reached.

2. Mathematical modeling of passive periodic mounts

2.1. Overview

Fig. 1a shows a schematic drawing of the shear mode passive periodic mount which is made of identical cells in the longitudinal direction. Each cell can be divided into four elements as shown in Fig. 1b. These elements are numbered 1,2,3, and 4 from the left to the right. The dynamic behavior of element 2 is dominated by the shear of the viscoelastic layer while elements 1, 3, and 4

* Corresponding author. Tel.: +1 301 405 5216; fax: +1 301 405 8331.
E-mail address: baz@umd.edu (A. Baz).

0168-874X/$ - see front matter © 2010 Elsevier B.V. All rights reserved.
doi:10.1016/j.finel.2010.03.007

Nomenclature

A	Area
b	width
E	Young's modulus of elasticity
F	Longitudinal traction force
G_2	Shear modulus of viscoelasticity
h_1,h_2,h_3	Thickness of core, viscoelastic material and outer layer
K_{ij}	The element of dynamic stiffness matrix of sub-cell
L_i	the length of sub-cell
m	Mass per unit length
N_i	Shape function of sub-cell
T	Kinetic energy
$\mathbf{T}$	Transfer matrix
u	Longitudinal deflection
V	Potential energy
W	External work
α_i	Coefficient of exponential shape function
α	Propagation attenuation factor
β	Propagation phase angle
γ	Shear strain
λ	Eigenvalues of the transfer matrix
δ_{ij}	Longitudinal deflection vector
ρ	Mass density
μ	Propagation parameter
ω	Frequency (rad/s)

Subscripts

jr, sk	nodes of element of core and outer layer, respectively.
x	Partial differential with respect to x
t	Partial differential with respect to t

Superscripts

-1	Matrix inverse

experience longitudinal loading. The transfer matrix of the unit cell is derived by applying the finite element approach along with the appropriate boundary conditions.

2.2. The transfer matrix of element 2

2.2.1. Main assumptions

(1) the shear strains in the metal core are negligible;
(2) the longitudinal stresses in the viscoelastic layer are negligible;
(3) the transverse displacements of all the points on any cross section of the periodic mount are not considered;
(4) the metal core and outer layers are assumed to be elastic and dissipate no energy;
(5) the viscoelastic layer is linearly viscoelastic.

2.2.2. Kinematic relationships

The deflected configuration is shown in Fig. 2 where A_1,E_1,h_1 denote the cross section area, Young's modulus and thickness of core. A_2,G_2,h_2,γ are the cross section area, shear's modulus,

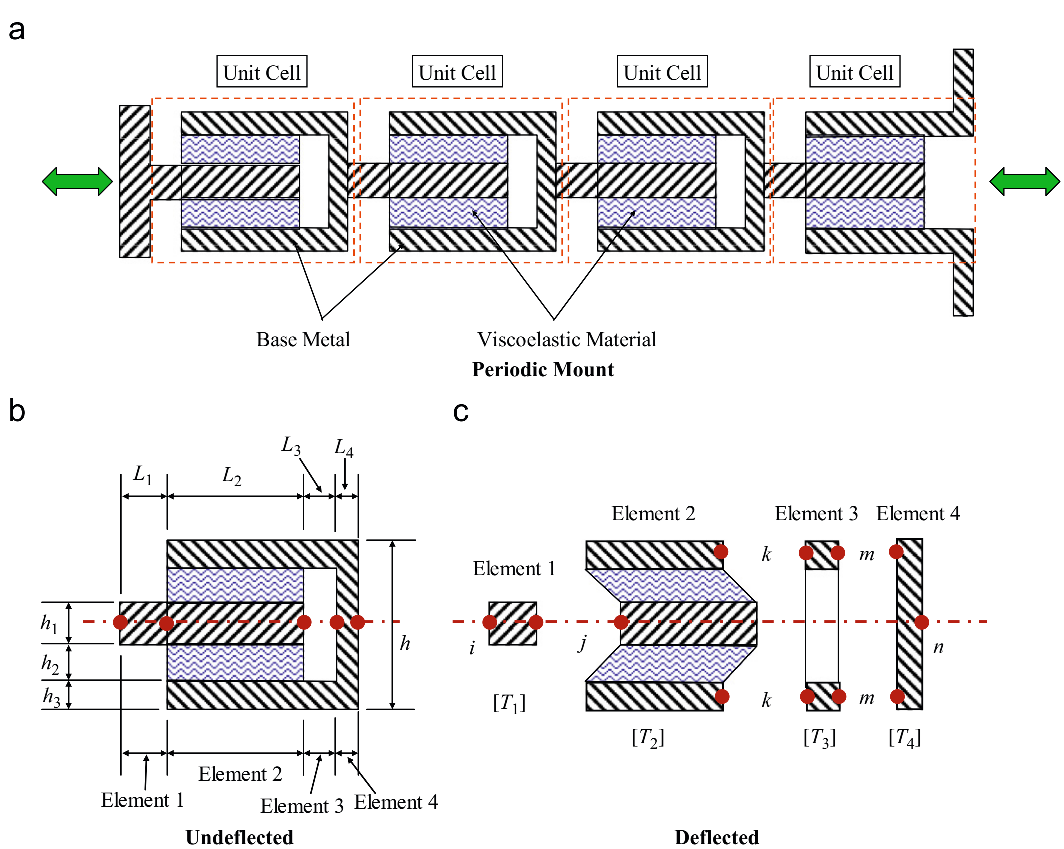

Fig. 1. Schematic drawing of shear mode periodic mount and main parameters: (a) periodic mount; (b) undeflected and (c) deflected.

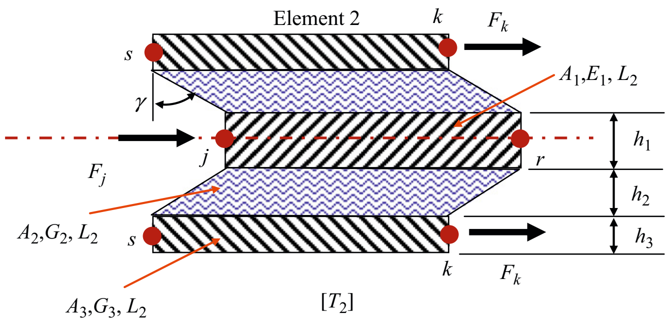

Fig. 2. Deflected configuration of Element 2.

thickness and shear strain of viscoelastic material. Also, A_3,E_3,h_3 define the cross section area, Young's modulus and thickness of outer layers.

From the geometry of Fig. 2, the shear strain γ in the viscoelastic material is given by

$$\gamma = (u_{jr} - u_{sk})/h_2 \tag{1}$$

where u_{jr} and u_{sk} are the longitudinal deflections of the core and outer layer, respectively. Also, h_2 defines the thickness of viscoelastic layer.

2.2.3. Energies of the element 2

Potential energies. The potential energies, V_1 and V_2, associated with the longitudinal extension of the core/outer layers and the shear of viscoelastic layers are given by

$$\begin{aligned} V = V_1 + V_2 &= \int\int\int_V \frac{1}{2}(\sigma_{jr}\varepsilon_{jr} + \sigma_{sk}\varepsilon_{sk} + \tau_2\gamma)dV \\ &= \frac{1}{2}E_1A_1\int_0^{L_2}\left(\frac{\partial u_{jr}}{\partial x}\right)^2 dx + \frac{1}{2}E_3A_3\int_0^{L_2}\left(\frac{\partial u_{sk}}{\partial x}\right)^2 dx \\ &\quad + \frac{1}{2}G_2A_2\int_0^{L_2}\gamma^2\,dx \end{aligned} \tag{2}$$

where $A_1 = h_1 b$, $A_2 = 2h_2 b$, $A_3 = 2h_3 b$ with b denoting the width of the core and the outer layer. Also, τ_2, G_2 denote shear stress and storage shear modulus of the viscoelastic layer. L_2 is the length of element 2. Subscripts jr, sk denote the nodes of the core and outer layer, respectively.

Kinetic energies. The kinetic energy T associated with the longitudinal deflection u_{jr} and u_{sk} is given by

$$T = \frac{1}{2}\rho_1A_1\int_0^{L_2}\left(\frac{\partial u_{jr}}{\partial t}\right)^2 dx + \frac{1}{2}\rho_3A_3\int_0^{L_2}\left(\frac{\partial u_{sk}}{\partial t}\right)^2 dx \tag{3}$$

where ρ_1, ρ_3 are the densities of the core and outer layer, respectively.

2.2.4. Finite element model of element 2

The displacements of core and outer layer can be described by the following shape functions:

$$\begin{aligned} u_{jr}(x) &= [N_j \;\; N_r]\begin{Bmatrix} u_j \\ u_r \end{Bmatrix} = [N_j \;\; N_r]\{\delta_{jr}\}, \\ u_{sk}(x) &= [N_s \;\; N_k]\begin{Bmatrix} u_s \\ u_k \end{Bmatrix} = [N_s \;\; N_k]\{\delta_{sk}\} \end{aligned} \tag{4}$$

where u_j,u_r,N_j,N_r are nodal displacements and shape functions at nodes j, r in core, as are u_s,u_k,N_s,N_k at nodes s, k of outer layer. From Eqs. (1) and (4), the shear strain γ becomes,

$$\gamma = (u_{jr} - u_{sk})/h_2 = (1/h_2)(N_ju_j + N_ru_r - N_su_s - N_ku_k)$$

$$= \left(\frac{1}{h_2}\right)\left(\left[\begin{array}{cc|cc} N_j & N_r & -N_s & -N_k \end{array}\right]\left\{\begin{array}{c} \delta_{jr} \\ \hline \delta_{sk} \end{array}\right\}\right) \tag{5}$$

u_{jr}, u_{sk} in Eq. (4) can be also rewritten as

$$u_{jr}(x) = \left[\begin{array}{cc|cc} N_j & N_r & 0 & 0 \end{array}\right]\left\{\begin{array}{c} \delta_{jr} \\ \hline \delta_{sk} \end{array}\right\}, \quad u_{sk}(x) = \left[\begin{array}{cc|cc} 0 & 0 & N_s & N_k \end{array}\right]\left\{\begin{array}{c} \delta_{jr} \\ \hline \delta_{sk} \end{array}\right\} \tag{6}$$

The potential energy of Eq. (2) can be evaluated using Eq. (6) as follows,

$$\begin{aligned} V &= \frac{1}{2}E_1A_1\int_0^{L_2}\left(\frac{\partial u_{jr}}{\partial x}\right)^T\left(\frac{\partial u_{jr}}{\partial x}\right)dx + \frac{1}{2}E_3A_3\int_0^{L_2}\left(\frac{\partial u_{sk}}{\partial x}\right)^T\left(\frac{\partial u_{sk}}{\partial x}\right)dx \\ &\quad + \frac{1}{2}G_2A_2\int_0^{L_2}(\gamma)^T(\gamma)dx = \frac{1}{2}\left\{\begin{array}{c} \delta_{jr} \\ \hline \delta_{sk} \end{array}\right\}^T([K_{jr}] + [K_{sk}] + [K_{vem}])\left\{\begin{array}{c} \delta_{jr} \\ \hline \delta_{sk} \end{array}\right\} \\ &= \frac{1}{2}\left\{\begin{array}{c} \delta_{jr} \\ \hline \delta_{sk} \end{array}\right\}^T[K_{ele2}]\left\{\begin{array}{c} \delta_{jr} \\ \hline \delta_{sk} \end{array}\right\} \end{aligned} \tag{7}$$

where

$$\begin{aligned} [K_{ele2}] = &\left(E_1A_1\int_0^{L_2}\left[\begin{array}{cc|cc} N_{j,x}N_{j,x} & N_{j,x}N_{r,x} & 0 & 0 \\ N_{r,x}N_{j,x} & N_{r,x}N_{r,x} & 0 & 0 \\ \hline 0 & 0 & 0 & 0 \\ 0 & 0 & 0 & 0 \end{array}\right]dx\right) \\ &+ \left(E_3A_3\int_0^{L_2}\left[\begin{array}{cc|cc} 0 & 0 & 0 & 0 \\ 0 & 0 & 0 & 0 \\ \hline 0 & 0 & N_{s,x}N_{s,x} & N_{s,x}N_{k,x} \\ 0 & 0 & N_{k,x}N_{s,x} & N_{k,x}N_{k,x} \end{array}\right]dx\right) \\ &+ \left(\left(\frac{G_2A_2}{h_2^2}\right)\int_0^{L_2}\left[\begin{array}{cc|cc} N_jN_j & N_jN_r & -N_jN_s & -N_jN_k \\ N_rN_j & N_rN_r & -N_rN_s & -N_rN_k \\ \hline -N_sN_j & -N_sN_r & N_sN_s & N_sN_k \\ -N_kN_j & -N_kN_r & N_kN_s & N_kN_k \end{array}\right]dx\right) \end{aligned}$$

One can also obtain mass matrix of element 2 using the kinetic energies,

$$\begin{aligned} T &= \frac{1}{2}\rho_1A_1\int_0^{L_2}\left(\frac{\partial u_{jr}}{\partial t}\right)^2 dx + \frac{1}{2}\rho_3A_3\int_0^{L_2}\left(\frac{\partial u_{sk}}{\partial t}\right)^2 dx \\ &= \frac{1}{2}\left\{\begin{array}{c} \dot{\delta}_{jr} \\ \hline \dot{\delta}_{sk} \end{array}\right\}^T\left([M_{jr}] + [M_{sk}]\right)\left\{\begin{array}{c} \dot{\delta}_{jr} \\ \hline \dot{\delta}_{sk} \end{array}\right\} = \frac{1}{2}\left\{\begin{array}{c} \dot{\delta}_{jr} \\ \hline \dot{\delta}_{sk} \end{array}\right\}^T[M_{ele2}]\left\{\begin{array}{c} \dot{\delta}_{jr} \\ \hline \dot{\delta}_{sk} \end{array}\right\} \end{aligned}$$

$$\begin{aligned} [M_{ele2}] = &\left(\rho_1A_1\int_0^{L_2}\left[\begin{array}{cc|cc} N_jN_j & N_jN_r & 0 & 0 \\ N_rN_j & N_rN_r & 0 & 0 \\ \hline 0 & 0 & 0 & 0 \\ 0 & 0 & 0 & 0 \end{array}\right]dx\right) \\ &+ \left(\rho_3A_3\int_0^{L_2}\left[\begin{array}{cc|cc} 0 & 0 & 0 & 0 \\ 0 & 0 & 0 & 0 \\ \hline 0 & 0 & N_sN_s & N_sN_k \\ 0 & 0 & N_kN_s & N_kN_k \end{array}\right]dx\right) \end{aligned} \tag{8}$$

The equation of motion for element 2 can be obtained as follows:

$$[M_{ele2}]\{\ddot{\delta}_{e2}\} + [K_{ele2}]\{\delta_{e2}\} = \{F_{ele2}\} \quad \text{or} \quad [K_{ele2}^D]\{\delta_{e2}\} = \{F_{ele2}\} \tag{9}$$

where dynamic stiffness $[K_{ele2}^D] = [K_{ele2} - \omega^2 M_{ele2}]$ and $\{\delta_{e2}\} = \{\delta_{jr}\;\; \delta_{sk}\}^T$. The dynamic stiffness matrix of element 2 can be given by

$$[K_{ele2}^D] = [K_{ele2} - \omega^2 M_{ele2}] = \left[\begin{array}{cc|cc} K_{jj} & K_{jr} & K_{js} & K_{jk} \\ K_{rj} & K_{rr} & K_{rs} & K_{rk} \\ \hline K_{sj} & K_{sr} & K_{ss} & K_{sk} \\ K_{kj} & K_{kr} & K_{ks} & K_{kk} \end{array}\right] \tag{10}$$

where

$$K_{ab}=\int_0^{L_2}[E_1A_1(N_{a,x}N_{b,x})+g(N_aN_b)-\omega^2\rho_1A_1(N_aN_b)]dx;\quad a=j,r;\;\; b=j,r$$

$$K_{js}=-\int_0^{L_2}[g(N_jN_s)]dx,\quad K_{jk}=-\int_0^{L_2}[g(N_jN_k)]dx,\quad K_{rs}=-\int_0^{L_2}[g(N_rN_s)]dx$$

$$K_{rk}=-\int_0^{L_2}[g(N_rN_k)]dx,\quad K_{sj}=-\int_0^{L_2}[g(N_sN_j)]dx,\quad K_{sr}=-\int_0^{L_2}[g(N_sN_r)]dx$$

$$K_{kj}=-\int_0^{L_2}[g(N_kN_j)]dx,\quad K_{kr}=-\int_0^{L_2}[g(N_kN_r)]dx$$

$$K_{cd}=\int_0^{L_2}[E_3A_3(N_{c,x}N_{d,x})+g(N_cN_d)-\omega^2\rho_3A_3(N_cN_d)]dx;\quad c=s,k;\; d=s,k$$

$$g=(G_2A_2/h_2^2)$$

2.2.5. The transfer matrix of element 2

The transfer matrix of element 2 can be obtained by using dynamic stiffness matrix of Eq. (10) and applying the free boundary condition at u_r, u_s:

$$\left[\begin{array}{cc|cc} K_{jj} & K_{jr} & K_{js} & K_{jk} \\ K_{rj} & K_{rr} & K_{rs} & K_{rk} \\ \hline K_{sj} & K_{sr} & K_{ss} & K_{sk} \\ K_{kj} & K_{kr} & K_{ks} & K_{kk} \end{array}\right]\begin{Bmatrix} u_j \\ u_r \\ u_s \\ u_k \end{Bmatrix}=\begin{Bmatrix} F_j \\ 0 \\ 0 \\ F_k \end{Bmatrix} \tag{11}$$

Rearranging Eq. (11) leads to the following equation:

$$\begin{bmatrix} K_{11}^{ele2} & K_{12}^{ele2} \\ K_{21}^{ele2} & K_{22}^{ele2} \end{bmatrix}\begin{Bmatrix} u_j \\ u_k \end{Bmatrix}=\begin{Bmatrix} F_j \\ F_k \end{Bmatrix} \tag{12}$$

From Eq. (12) and Fig. 2, one can establish the transfer matrix $[\mathbf{T}_2]$:

$$\begin{Bmatrix} u_{j+1} \\ F_{j+1} \end{Bmatrix}=\begin{Bmatrix} u_k \\ -F_k \end{Bmatrix}=[\mathbf{T}_2]\begin{Bmatrix} u_j \\ F_j \end{Bmatrix} \tag{13}$$

where $[\mathbf{T}_2]$ is the transfer matrix of element 2. Combining Eq. (12) and (13) yields the transfer matrix $[\mathbf{T}_2]$:

$$\begin{bmatrix} u_k \\ F_k \end{bmatrix}=\left[\begin{array}{c|c} -\left(K_{12}^{ele2}\right)^{-1}\left(K_{11}^{ele2}\right) & \left(K_{12}^{ele2}\right)^{-1} \\ \hline \left(K_{22}^{ele2}\right)\left(K_{12}^{ele2}\right)^{-1}\left(K_{11}^{ele2}\right)-\left(K_{21}^{ele2}\right) & -\left(K_{22}^{ele2}\right)\left(K_{12}^{ele2}\right)^{-1} \end{array}\right]\begin{bmatrix} u_j \\ F_j \end{bmatrix} \tag{14}$$

or

$$[\mathbf{T}_2]=\left[\begin{array}{c|c} -\left(K_{12}^{ele2}\right)^{-1}\left(K_{11}^{ele2}\right) & \left(K_{12}^{ele2}\right)^{-1} \\ \hline \left(K_{22}^{ele2}\right)\left(K_{12}^{ele2}\right)^{-1}\left(K_{11}^{ele2}\right)-\left(K_{21}^{ele2}\right) & -\left(K_{22}^{ele2}\right)\left(K_{12}^{ele2}\right)^{-1} \end{array}\right] \tag{15}$$

where

$$K_{11}^{ele2}=(K_{jj})+(K_{js})C_j+(K_{jr})D_j,\quad K_{12}^{ele2}=(K_{jk})+(K_{js})C_k+(K_{jr})D_k$$

$$K_{21}^{ele2}=(K_{kj})+(K_{ks})C_j+(K_{kr})D_j,\quad K_{22}^{ele2}=(K_{kk})+(K_{ks})C_k+(K_{kr})D_k$$

$$C_j=-[(K_{ss})-(K_{sr})(K_{rr})^{-1}(K_{rs})]^{-1}[(K_{sj})-(K_{sr})(K_{rr})^{-1}(K_{rj})]$$

$$C_k=-[(K_{ss})-(K_{sr})(K_{rr})^{-1}(K_{rs})]^{-1}[(K_{sk})-(K_{sr})(K_{rr})^{-1}(K_{rk})]$$

$$D_j=[-(K_{rr})^{-1}(K_{rj})-(K_{rr})^{-1}(K_{rs})C_j]$$

$$D_k=[-(K_{rr})^{-1}(K_{rk})-(K_{rr})^{-1}(K_{rs})C_k]$$

2.3. The transfer matrices of elements 1, 3 and 4

Elements 1,3 and 4 can be regarded as one-dimensional rod with different cross section areas, therefore, their potential and kinetic energies have the similar form:

$$V_i=\frac{1}{2}E_iA_i\int_0^{L_i}\left(\frac{\partial u_i}{\partial x}\right)^2dx, \tag{16}$$

$$T_i=\frac{1}{2}\rho_iA_i\int_0^{L_i}\left(\frac{\partial u_i}{\partial t}\right)^2dx,\quad i=1,3,4 \tag{17}$$

Let u_1, u_2 be the axial displacement of two nodes of one element. Also Let $N_1(x)$,$N_2(x)$ be the shape function of u_1, u_2. The deflection variation of one-dimensional rod can be derived as

$$u_i(x)=[N_1(x)\;\;N_2(x)]\begin{Bmatrix} u_1 \\ u_2 \end{Bmatrix}=[N][\delta_e] \tag{18}$$

where $\{\delta_e\}=\{u_1\;\;u_2\}^T$. One can evaluate potential energies and kinetic energies as follows:

$$\begin{aligned} V_i&=\frac{1}{2}E_iA_i\int_0^{L_i}\left(\frac{\partial u_i}{\partial x}\right)^T\left(\frac{\partial u_i}{\partial x}\right)dx \\ &=\frac{1}{2}\left\{\delta_e\right\}^T\left(E_iA_i\int_0^{L_i}\begin{bmatrix} \frac{\partial N_1}{\partial x}\frac{\partial N_1}{\partial x} & \frac{\partial N_1}{\partial x}\frac{\partial N_2}{\partial x} \\ \frac{\partial N_2}{\partial x}\frac{\partial N_1}{\partial x} & \frac{\partial N_2}{\partial x}\frac{\partial N_2}{\partial x} \end{bmatrix}dx\right)\{\delta_e\} \\ &=\frac{1}{2}\left\{\delta_e\right\}^T[k_a^i]\{\delta_e\} \end{aligned} \tag{19}$$

$$\begin{aligned} T_i&=\frac{1}{2}\rho_iA_i\int_0^{L_i}\left(\frac{\partial u_i}{\partial t}\right)^T\left(\frac{\partial u_i}{\partial t}\right)dx \\ &=\frac{1}{2}\left\{\dot{\delta}_e\right\}^T\left(\rho_iA_i\int_0^{L_i}\begin{bmatrix} N_1N_1 & N_1N_2 \\ N_2N_1 & N_2N_2 \end{bmatrix}dx\right)\left\{\dot{\delta}_e\right\}=\frac{1}{2}\left\{\dot{\delta}_e\right\}^T[m_a^i]\left\{\dot{\delta}_e\right\} \end{aligned} \tag{20}$$

The equation of motion for one element can be obtained as follows:

$$[m_a^i]\{\ddot{\delta}_e\}+[k_a^i]\{\delta_e\}=\{F_e\}\quad\text{or}\quad[k_a^i-\omega^2m_a^i]\{\delta_e\}=\{F_e\} \tag{21}$$

From Eq. (21), the dynamic matrix of elements 1,3, and 4 are given by

$$[k_D^i]=\begin{bmatrix} E_iA_i\int_0^{L_i}\left\{\frac{\partial N_1}{\partial x}\frac{\partial N_1}{\partial x}-\omega^2\left(\frac{\rho_i}{E_i}\right)(N_1N_1)\right\}dx & E_iA_i\int_0^{L_i}\left\{\frac{\partial N_1}{\partial x}\frac{\partial N_2}{\partial x}-\omega^2\left(\frac{\rho_i}{E_i}\right)(N_1N_2)\right\}dx \\ E_iA_i\int_0^{L_i}\left\{\frac{\partial N_2}{\partial x}\frac{\partial N_1}{\partial x}-\omega^2\left(\frac{\rho_i}{E_i}\right)(N_2N_1)\right\}dx & E_iA_i\int_0^{L_i}\left\{\frac{\partial N_2}{\partial x}\frac{\partial N_2}{\partial x}-\omega^2\left(\frac{\rho_i}{E_i}\right)(N_2N_2)\right\}dx \end{bmatrix} \tag{22}$$

From Eq. (21), the equation of motion of an element can be expressed as follows:

$$[k_D^i]\begin{Bmatrix} u_1^i \\ u_2^i \end{Bmatrix}=\begin{Bmatrix} F_1^i \\ F_2^i \end{Bmatrix}\quad\text{or}\quad\begin{bmatrix} k_{11}^i & k_{12}^i \\ k_{21}^i & k_{22}^i \end{bmatrix}\begin{Bmatrix} u_1^i \\ u_2^i \end{Bmatrix}=\begin{Bmatrix} F_1^i \\ F_2^i \end{Bmatrix} \tag{23}$$

Table 1
Geometric properties.

Length (mm)		Thickness (mm)		Width (mm)	
L_1	4.76	h_1	3.17	b	25.4
L_2	17.46	h_2	3.18, 8, 15		
L_3	4.76				
L_4	4.76	h_3	3.18		

Table 2
Physical properties.

Material	Density (kg m^{-3})	Modulus (MPa)
Aluminum	2700	70 000[a]
Viscoelastic layer	1200	$15+0.0i$[b]

[a] Young's modulus.
[b] Complex shear modulus($G(1+\eta i)$, $\eta=0.0$).

The transfer matrix $[T_i]$ between (i)th element and $(i+1)$th element has the following relationship,

$$\begin{Bmatrix} u_1^{i+1} \\ F_1^{i+1} \end{Bmatrix} = \begin{Bmatrix} u_2^{i} \\ -F_2^{i} \end{Bmatrix} = [\mathbf{T}_i]\begin{Bmatrix} u_1^{i} \\ F_1^{i} \end{Bmatrix} \tag{24}$$

Combining Eqs. (23) and (24) gives the transfer matrix as follows:

$$[\mathbf{T}_i] = \left[\begin{array}{c:c} -(k_{12}^i)^{-1}(k_{11}^i) & (k_{12}^i)^{-1} \\ \hdashline (k_{22}^i)(k_{12}^i)^{-1}(k_{11}^i)-(k_{21}^i) & -(k_{22}^i)(k_{12}^i)^{-1} \end{array}\right], \quad i=1,3,4 \tag{25}$$

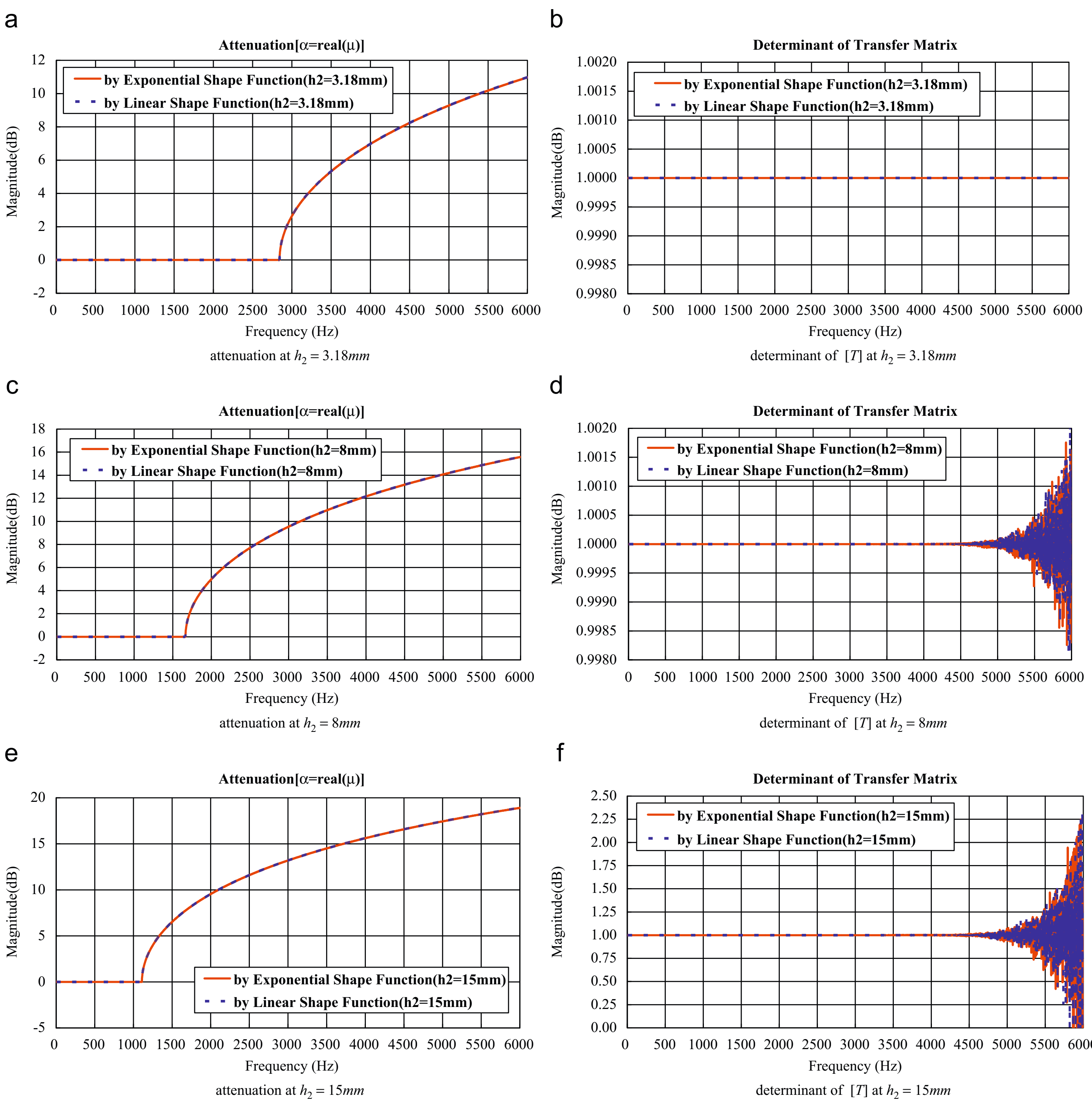

Fig. 3. The propagation constant and determinant of $[T]$ for passive periodic shear mode mount using exponential and linear shape functions for element 2: (a) attenuation at $h_2=3.18$ mm; (b) determinant of $[T]$ at $h_2=3.18$ mm; (c) attenuation at $h_2=8$ mm; (d) determinant of $[T]$ at $h_2=8$ mm; (e) attenuation at $h_2=15$ mm and (f) determinant of $[T]$ at $h_2=15$ mm.

2.4. The transfer matrix of the passive periodic mount

Now, the transfer matrix of unit cell can be computed as

$$\mathbf{T}_{cell} = [\mathbf{T}_{element4}] \times [\mathbf{T}_{element3}] \times [\mathbf{T}_{element2}] \times [\mathbf{T}_{element1}] \tag{26}$$

and for the complete periodic mount

$$\mathbf{T} = (\mathbf{T}_{cell})^{N_{cell}} \tag{27}$$

where N_{cell} is the number of cells in the passive periodic mount. Thus, all the information about the propagation characteristics is given by the eigenvalues λ of the transfer matrix $\mathbf{T}$:

$$\lambda = e^{\mu} = e^{\alpha + \beta i} \tag{28}$$

where μ is the propagation constants, α and β are called attenuation factor and phase angle and represent the real and imaginary portion of the propagation constant. Also, one another important characteristic of the transfer matrix T is

$$\textit{Determinant of } [\mathbf{T}] = 1 \tag{29}$$

This can be proved using Eq. (15) and the symmetry of the dynamic stiffness matrix:

$$\det[\mathbf{T}_2] = \det\left[\begin{array}{c:c} -(K_{12}^{ele2})^{-1}(K_{11}^{ele2}) & (K_{12}^{ele2})^{-1} \\ \hdashline (K_{22}^{ele2})(K_{12}^{ele2})^{-1}(K_{11}^{ele2}) - (K_{21}^{ele2}) & -(K_{22}^{ele2})(K_{12}^{ele2})^{-1} \end{array}\right]$$
$$= \det[(K_{12}^{ele2})^{-1}(K_{21}^{ele2})^{T}] = \det[(K_{12}^{ele2})^{-1}(K_{12}^{ele2})] = \det[I] = 1 \tag{30}$$

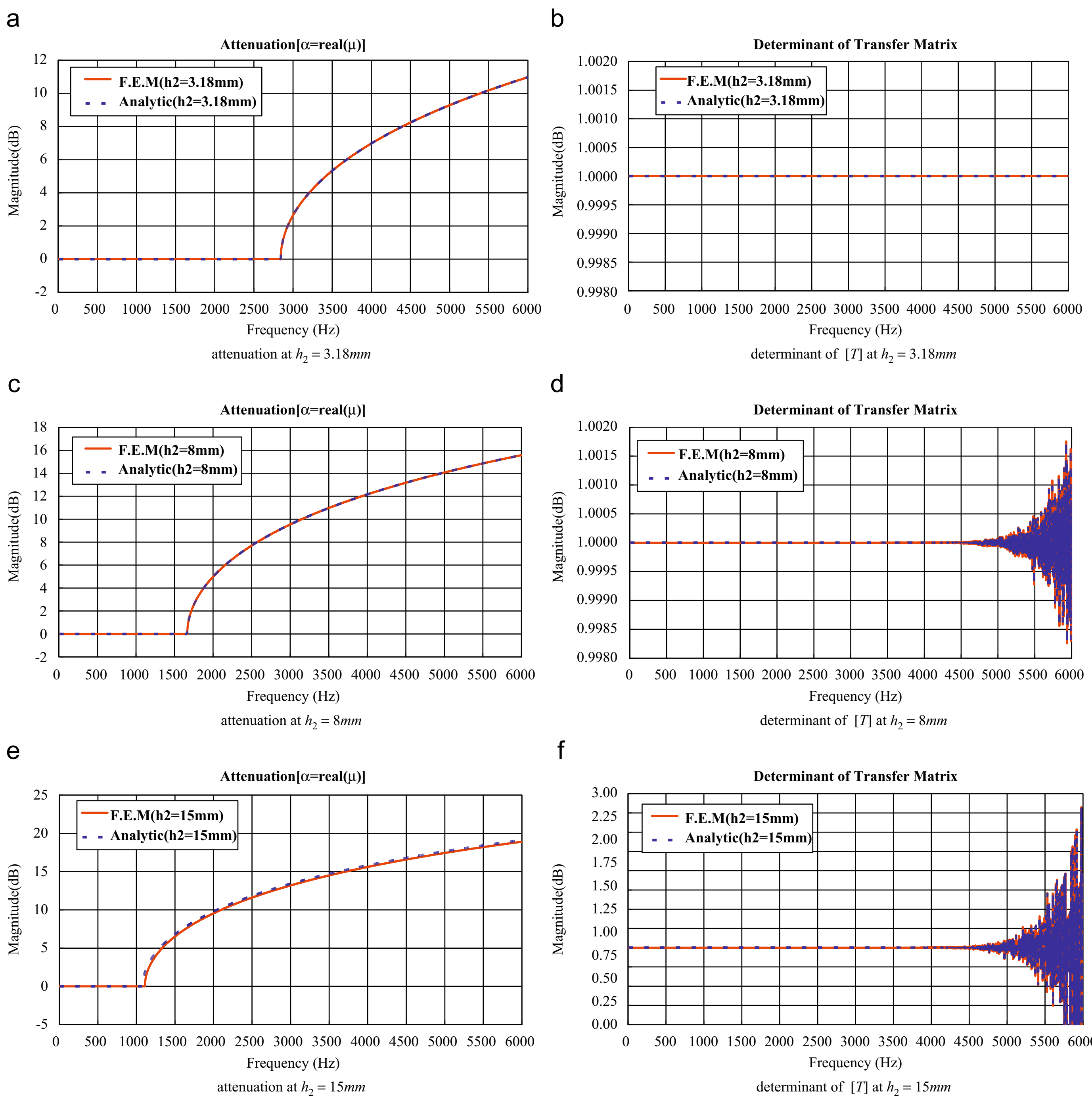

Fig. 4. The propagation constant and determinant of [T]for passive periodic shear mode mount using F.E.M and analytical method [28]: (a) attenuation at h_2=3.18 mm; (b) determinant of [T] at h_2=3.18 mm; (c) attenuation at h_2=8 mm; (d) determinant of [T] at h_2=8 mm; (e) attenuation at h_2=15 mm and (f) determinant of [T] at h_2=15 mm.

Eq. (30) can be used effectively for checking the accuracy of transfer matrix **T**.

3. Performance of passive periodic mount

3.1. Shape function of element 2 and elements 1, 3, 4

The one-dimensional rod element has two nodes and one degree of freedom at each node, the axial displacement can be represented by exponential function which is derived from the equation of longitudinal vibration in a rod and also is suitable in the higher frequency range:

$$u_i(x) = Ae^{-jk_ix} + Be^{jk_ix} = [e^{-jk_ix} \;\; e^{jk_ix}]\begin{bmatrix} A \\ B \end{bmatrix} \tag{31}$$

where $k_i^2 = (\rho_i/E_i)\omega^2$, ω is the exciting frequency(rad/s). Applying boundary conditions $u_i(0) = u_1$ at $x=0$ and $u_i(L_i) = u_2$ at $x=L_i$ and solving A, B yield

$$\begin{Bmatrix} A \\ B \end{Bmatrix} = \frac{1}{(e^{jk_iL_i} - e^{-jk_iL_i})}\begin{bmatrix} e^{jk_iL_i} & -1 \\ -e^{-jk_iL_i} & 1 \end{bmatrix}\begin{Bmatrix} u_1 \\ u_2 \end{Bmatrix} = \alpha_i\begin{bmatrix} e^{jk_iL_i} & -1 \\ -e^{-jk_iL_i} & 1 \end{bmatrix}\begin{Bmatrix} u_1 \\ u_2 \end{Bmatrix} \tag{32}$$

Substituting Eq. (32) into Eq. (31) leads to

$$u_i(x) = \alpha_i[e^{jk_i(L_i-x)} - e^{-jk_i(L_i-x)} \;\; e^{jk_ix} - e^{-jk_ix}]\begin{Bmatrix} u_1 \\ u_2 \end{Bmatrix} = [N_p(x) \;\; N_q(x)]\begin{Bmatrix} u_1 \\ u_2 \end{Bmatrix} = [N]\{\delta_e\} \tag{33}$$

From Eq. (33), N_j, N_r, N_s, N_k of element 2 and N_1, N_2 of element 1,3,4 are expressed as

$$N_p(x) = \alpha_p[e^{jk_p(L_p-x)} - e^{-jk_p(L_p-x)}], \quad p = j,s,1$$

$$N_q(x) = \alpha_q[e^{jk_qx} - e^{-jk_qx}], \quad q = r,k,2 \tag{34}$$

In addition to the exponential shape functions of Eq. (34), linear shape functions for element 2 are also used to obtain the mechanical filtering characteristics of passive periodic shear mode mount.

$$u_i(x) = [1 \;\; x]\begin{Bmatrix} A \\ B \end{Bmatrix} = [1 \;\; x]\begin{bmatrix} 1 & 0 \\ -1/L_i & 1/L_i \end{bmatrix}\begin{Bmatrix} u_1 \\ u_2 \end{Bmatrix} = \begin{bmatrix} \dfrac{L_i - x}{L_i} & \dfrac{x}{L_i} \end{bmatrix}\begin{Bmatrix} u_1 \\ u_2 \end{Bmatrix} = [N_m \;\; N_n]\{\delta_e\} = [N]\{\delta_e\} \tag{35}$$

From Eq. (35),

$$N_m(x) = 1 - (x/L_m), \quad m = j,s$$

$$N_n(x) = (x/L_n), \quad n = r,k \tag{36}$$

3.2. Materials

The passive periodic mount is made of two materials, one is aluminum, and the other is rubber as shown in Fig. 1. The geometric and physical properties of them are given in Tables 1 and 2.

3.3. The propagation of waves in passive periodic mount

3.3.1. The comparison between exponential and linear shape function

Fig. 3 shows comparisons between the filtering characteristics of the passive periodic shear mode mount with four cells when the shape function of element 2 is exponential and linear. From Fig. 3, it is evident that there is no difference between exponential and linear shape function of element 2. In this paper, exponential shape function is used for calculation of the propagation characteristics.

3.3.2. Comparison between F.E.M and analytic approach

Fig. 4 displays comparisons between the filtering characteristic of the passive periodic shear mount with four cells as predicted by the F.E.M and analytical method suggested by the authors [24]. Accordingly, the F.E.M will be used to calculate the propagation characteristics of the passive periodic shear mount.

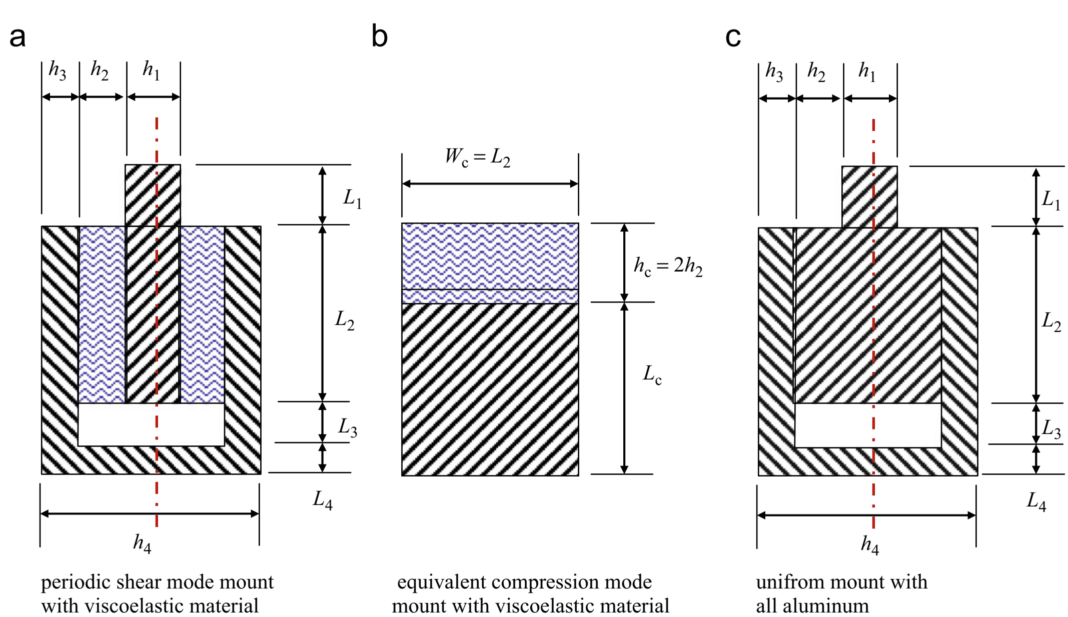

Fig. 5. Drawing of the cell of the passive periodic shear, equivalent compression and uniform mounts

3.3.3. Comparison between shear and compression mount

Fig. 5 shows unit cells of the passive periodic shear mount, equivalent compression and uniform mount, respectively. The dimensions of the equivalent passive periodic compression mount are determined to maintain the same dimension of the viscoelastic material as the shear mount and have the same cross section of the aluminum parts in both mounts, namely by,

$$h_c = 2h_2, \quad W_c = L_2, \quad L_c = h_1(L_1 + L_2) + 2h_3(L_2 + L_3) + h_4 L_4 \tag{37}$$

Fig. 6 shows the attenuation factor of the propagation constant, respectively, for the shear, compression, and uniform mount configurations. It can be seen that the compression mount is more effective than the shear mount when the thickness of the viscoelastic layer is small (Fig. 6a). However, increasing the thickness of the viscoelastic layer makes the passive periodic shear mount exhibit broader stop band characteristics than the compression mount (Fig. 6c). It should also be noted that stop bands are not observed over the entire frequency range for the uniform aluminum mount. This result emphasizes that the transmission of the vibration along the passive periodic mount is blocked over certain frequency bands by virtue of the periodicity effect.

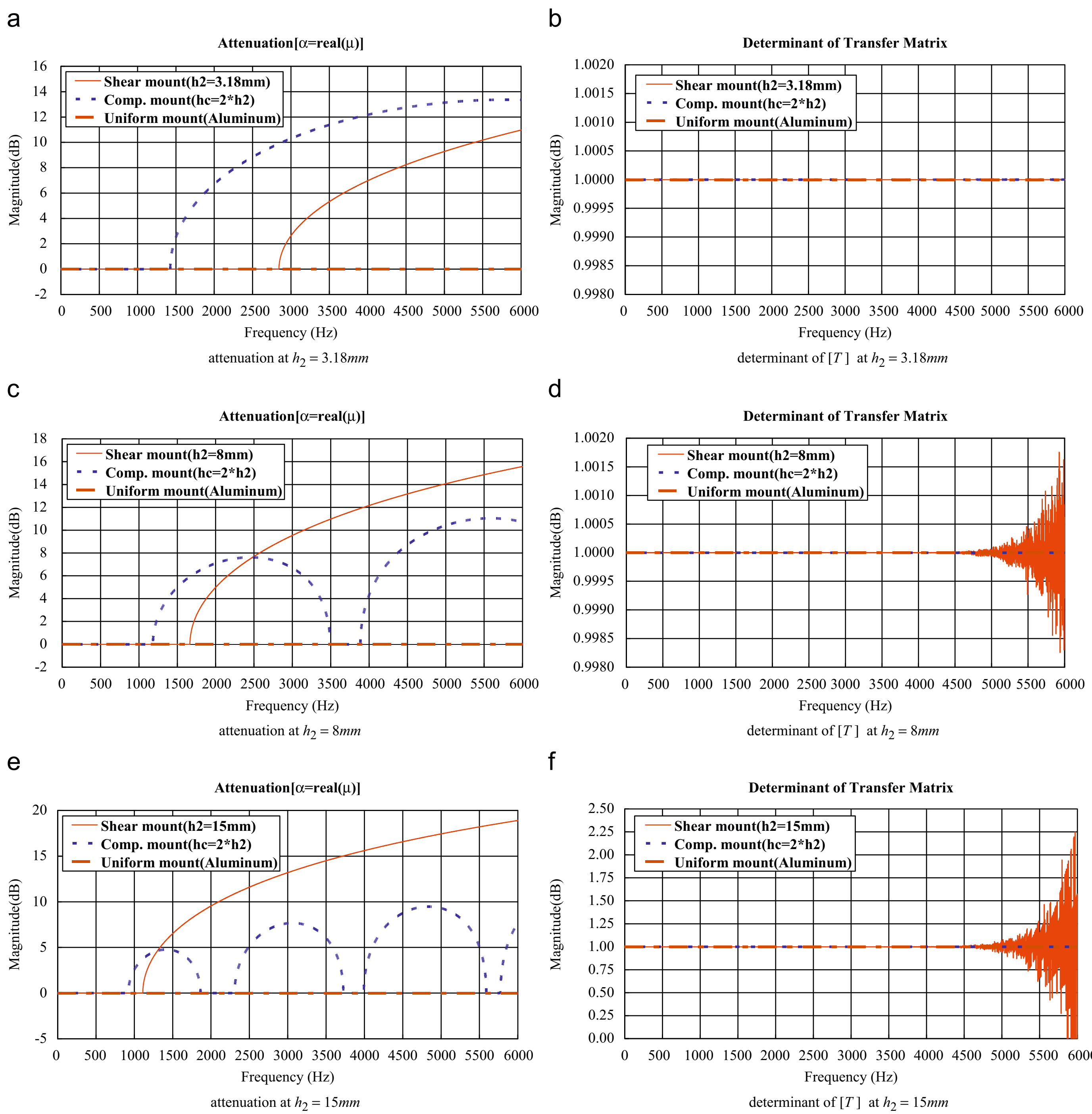

Fig. 6. The propagation constant and determinant of [T]for passive periodic shear mode, equivalent compression mode and uniform mounts: (a) attenuation at h_2=3.18 mm; (b) determinant of [T] at h_2==3.18 mm; (c) attenuation at h_2==8 mm; (d) determinant of [T] at h_2=8 mm; (e) attenuation at h_2=15 mm and (f) determinant of [T] at h_2=15 mm.

Fig. 7 displays a numerical comparison between the transmissibility of the passive periodic shear, equivalent compression and uniform mode mounts. It can be seen that a significant attenuation of vibration transmission occurs over the zones of the stop bands. More importantly, it can be seen that the shear mode mount, with thicker viscoelastic layers, is more effective than the compression mode mount. The reverse is true for thinner viscoelastic layers.

4. Experimental performance of periodic mount

In order to validate the predictions of theoretical model, a series of experiments are performed. Two experimental prototypes of mounts are designed and manufactured. One prototype is used to measure the amplitude of the transfer function the passive periodic mount, the other is used to determine the transfer function of a conventional non-periodic mount. Fig. 8

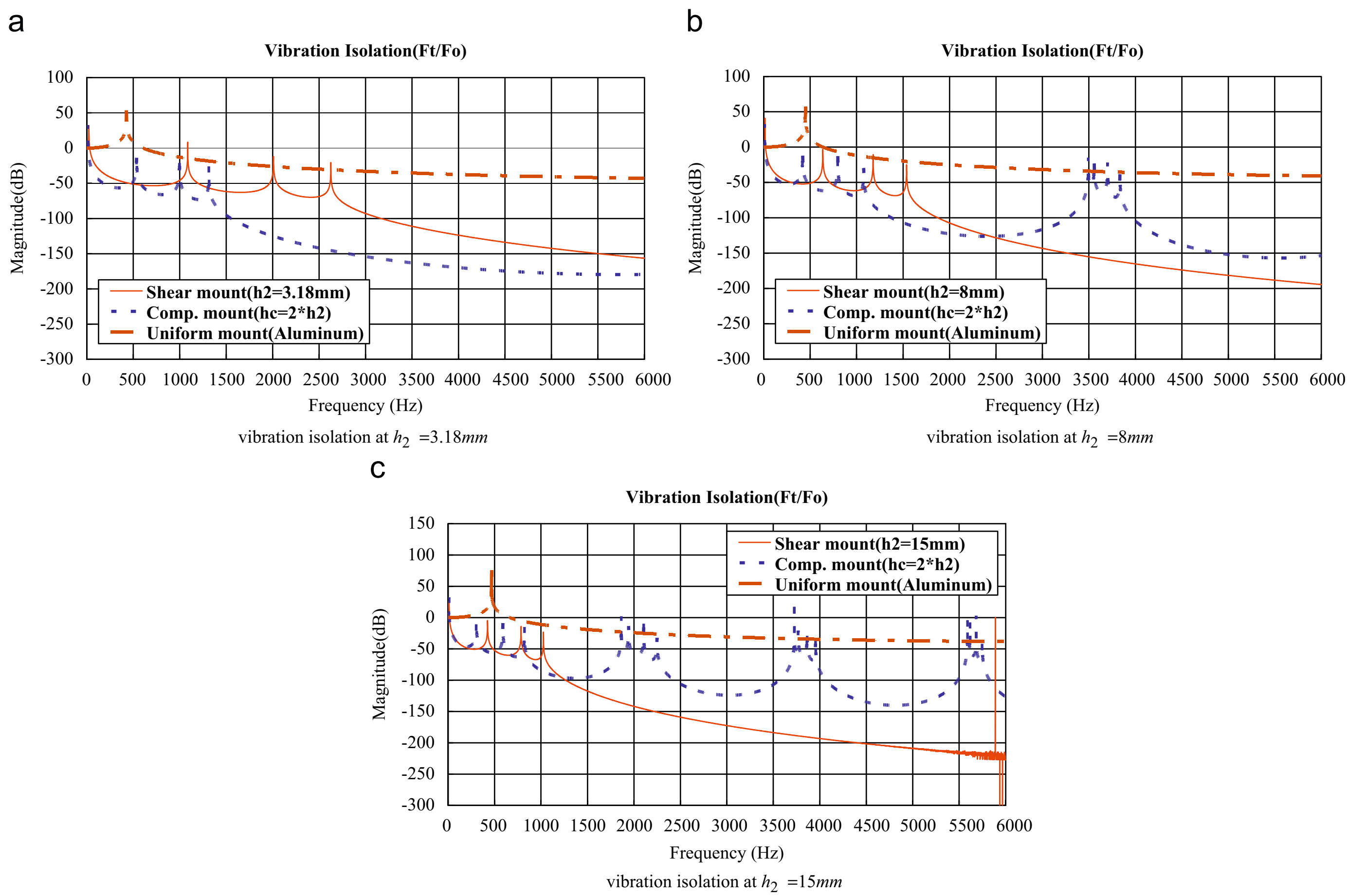

Fig. 7. Theoretical amplitude of the vibration isolation of periodic and uniform mounts: (a) vibration isolation at $h_2 = 3.18$ mm; (b) vibration isolation at $h_2 = 8$ mm and (c) vibration isolation at $h_2 = 15$ mm.

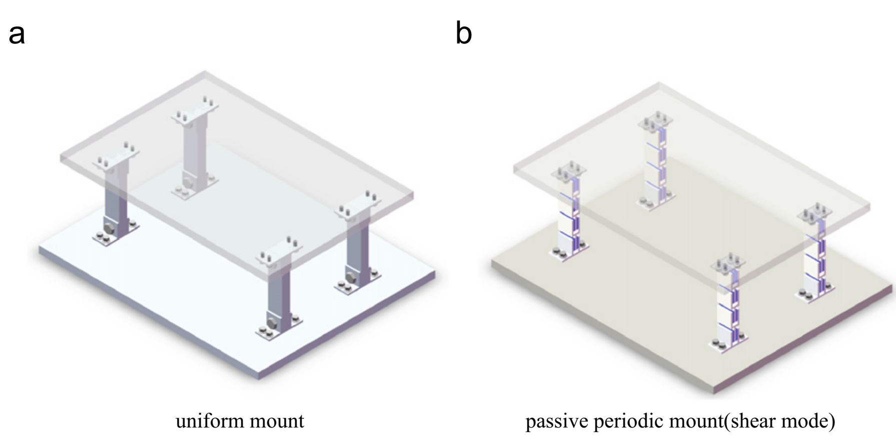

Fig. 8. Experimental models of uniform and passive periodic mounts: (a) uniform mount and (b) passive periodic mount (shear mode).

shows schematic drawings of the two prototypes and Fig. 9 shows a photograph of the experimental periodic mount. It can be seen that the prototype with four passive periodic mounts is used to measure the vibration transmission from the upper plate which is excited by a shaker. Each periodic mount is made of four cells. Piezoelectric accelerometers (PCB Model 303A3) are placed at the ends of the passive periodic mount. An accelerometer is used to measure the acceleration produced by the shaker at the top of the mount while the other accelerometer is used to capture acceleration transmitted to the bottom of the mount. A spectrum analyzer (ONO SOKKI Model CF910) is used to record the output signals of the accelerometers.

The predictions of the developed model are also validated against the predictions of the commercially available finite element package ANSYS. Fig. 10 displays ANSYS finite element model of the passive periodic mount. Also, the predictions of the ANSYS model are validated against the experimental results.

Fig. 11 shows a comparison between the amplitude of the experimental transfer functions relating the input excitation of the top end of the mount to transmitted acceleration to its other end. Fig. 12 shows the corresponding numerical transfer function as obtained by using ANSYS. It can be clearly seen that the stop bands cover the whole frequency range from the low frequencies to high frequencies. The attenuation of the vibration transmission is obvious and effective over the entire frequency range.

It is also evident that the experimental results are in agreement with the prediction of theoretical model in Section 3 and those obtained from numerical analysis using ANSYS.

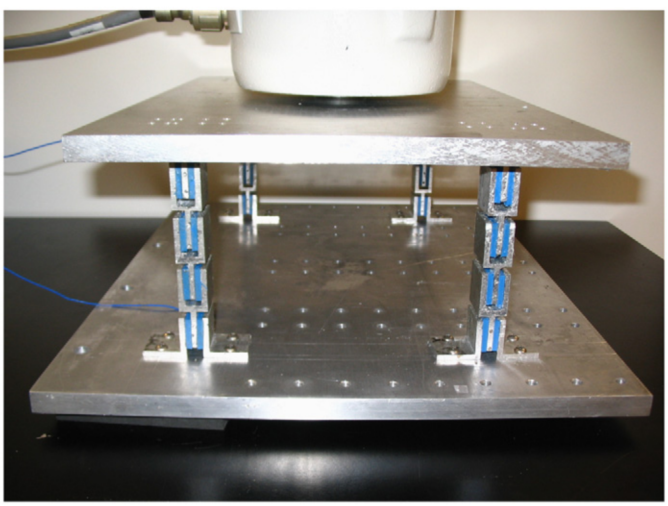

Fig. 9. The experimental passive periodic shear mode mount.

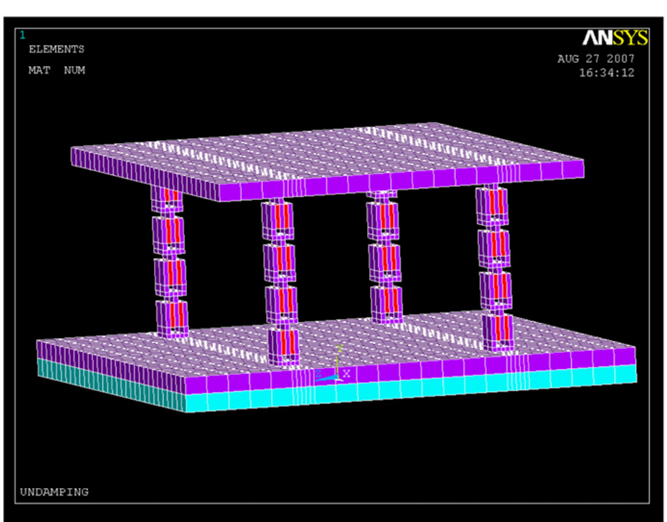

Fig. 10. ANSYS finite element model of the passive periodic shear mode mount.

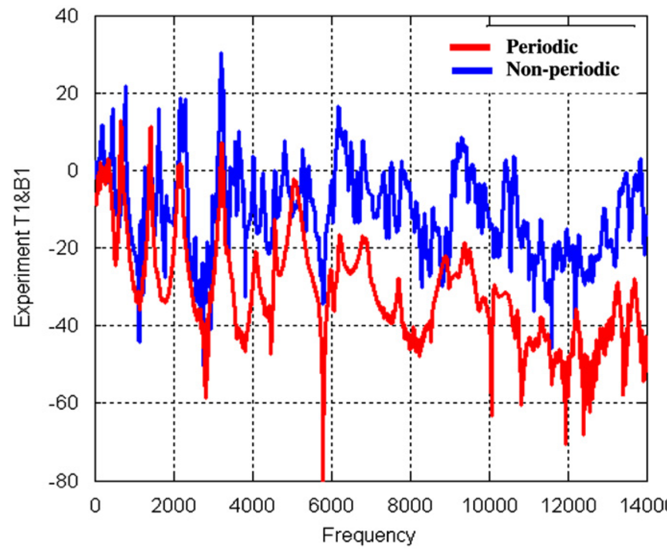

Fig. 11. Amplitude of the experimental transfer function.

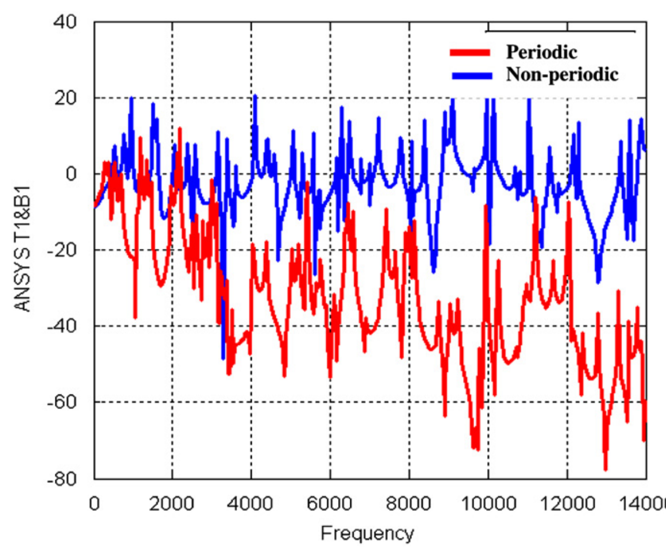

Fig. 12. Amplitude of the ANSYS transfer function.

5. Conclusions

In this study, a passive periodic engine mount with periodic viscoelastic inserts is presented. A theoretical model is developed to describe the dynamics of wave propagation in the passive periodic mount. The model is derived using the theory of finite elements. A cell of the passive periodic mount is divided into four elements, the transfer matrix formulation for each element is given. The overall transfer matrix of unit cell is obtained by multiplying the transfer matrices of the four elements composing the cell. The mechanical filtering characteristics of wave propagation in four series cells thus are analyzed by the transfer matrix formulation.

Numerical examples are given to illustrate the effectiveness of this class of periodic mounts. The experiments are performed to validate the predictions of the theoretical model. Both the theoretical and experimental results show that the passive periodic mount exhibit stop bands covering a broad frequency range.

The presented engine mounts can find many applications in gearbox support struts, engine mounts of automobiles and aircraft as well as underwater vehicles. The development of active prototypes of the shear mode periodic mount presented here is a natural extension of the present work.

Appendix A. Element of matrix in Eq. (10)

A.1. Exponential shape function

Exponential shape function can be Eq. (A.1):

$$N_j=\alpha_1[e^{jk_1(L_2-x)}-e^{-jk_1(L_2-x)}],\quad N_{j,x}=\alpha_1(-jk_1)[e^{jk_1(L_2-x)}+e^{-jk_1(L_2-x)}],$$

$$N_r=\alpha_1(e^{jk_1x}-e^{-jk_1x}),\quad N_{r,x}=\alpha_1(jk_1e^{jk_1x}+jk_1e^{-jk_1x})=\alpha_1(jk_1)(e^{jk_1x}+e^{-jk_1x})$$

$$N_s=\alpha_3[e^{jk_3(L_2-x)}-e^{-jk_3(L_2-x)}],\quad N_{s,x}=\alpha_3(-jk_3)[e^{jk_3(L_2-x)}+e^{-jk_3(L_2-x)}],$$

$$N_k=\alpha_3(e^{jk_3x}-e^{-jk_3x}),\quad N_{k,x}=\alpha_3(jk_3e^{jk_3x}+jk_3e^{-jk_3x})=\alpha_3(jk_3)(e^{jk_3x}+e^{-jk_3x})$$

$$\alpha_1=\frac{1}{(e^{jk_1L_2}-e^{-jk_1L_2})},\quad \alpha_3=\frac{1}{(e^{jk_3L_2}-e^{-jk_3L_2})},\quad k_i^2=(\rho_i/E_i)\omega^2 \tag{A.1}$$

Inserting exponential shape function in (A.1) into Eq. (10) gives

$$\begin{aligned}K_{jj}&=\int_0^{L_2}[E_1A_1(N_{j,x}N_{j,x})+g(N_jN_j)-\omega^2\rho_1A_1(N_jN_j)]dx\\&=\left(\frac{E_1A_1}{L_2}\right)\left[\frac{(1-e^{-j4k_1L_2})}{(1-e^{-j2k_1L_2})^2}\right](jk_1L_2)+g\alpha_1^2\left[-2L_2-j\left(\frac{1}{2k_1}\right)(e^{j2k_1L_2}-e^{-j2k_1L_2})\right]\end{aligned}$$

$$K_{jr}=\int_0^{L_2}[E_1A_1(N_{j,x}N_{r,x})+g(N_jN_r)-\omega^2\rho_1A_1(N_jN_r)]dx=-\left(\frac{E_1A_1}{L_2}\right)\left[\frac{2e^{-j3k_1L_2}(-1+e^{j2k_1L_2})}{(1-e^{-j2k_1L_2})^2}\right](jk_1L_2)+g\alpha_1^2\left[(e^{jk_1L_2}+e^{-jk_1L_2})L_2+j\left(\frac{1}{k_1}\right)(e^{jk_1L_2}-e^{-jk_1L_2})\right]$$

$$K_{js}=-g\int_0^{L_2}[(N_jN_s)]dx=\begin{cases}g\alpha_1\alpha_3(j)\left[\left(\frac{1}{k_1+k_3}\right)(e^{j(k_1+k_3)L_2}-e^{-j(k_1+k_3)L_2})-\left(\frac{1}{k_1-k_3}\right)(e^{j(k_1-k_3)L_2}-e^{-j(k_1-k_3)L_2})\right], & k_1\neq k_3\\ g(\alpha_\alpha)^2\left[2L_2+j\left(\frac{1}{2k_\alpha}\right)(e^{j2k_\alpha L_2}-e^{-j2k_\alpha L_2})\right], & k_1=k_3=k_\alpha\end{cases}$$

$$K_{jk}=-g\int_0^{L_2}[(N_jN_k)]dx=\begin{cases}g\alpha_1\alpha_3(j)\left(\frac{2k_1}{(k_1^2-k_3^2)}\right)[(e^{jk_1L_2}-e^{-jk_1L_2})-(e^{jk_3L_2}-e^{-jk_3L_2})], & k_1\neq k_3\\ g(\alpha_\alpha)^2\left[-(e^{jk_\alpha L_2}+e^{-jk_\alpha L_2})L_2-j\left(\frac{1}{k_\alpha}\right)(e^{jk_\alpha L_2}-e^{-jk_\alpha L_2})\right], & k_1=k_3=k_\alpha\end{cases}$$

$$K_{rj}=\int_0^{L_2}[E_1A_1(N_{r,x}N_{j,x})+g(N_rN_j)-\omega^2\rho_1A_1(N_rN_j)]dx=-\left(\frac{E_1A_1}{L_2}\right)\left[\frac{2e^{-j3k_1L_2}(-1+e^{j2k_1L_2})}{(1-e^{-j2k_1L_2})^2}\right](jk_1L_2)+g\alpha_1^2\left[(e^{jk_1L_2}+e^{-jk_1L_2})L_2+j\left(\frac{1}{k_1}\right)(e^{jk_1L_2}-e^{-jk_1L_2})\right]$$

$$K_{rr}=\int_0^{L_2}[E_1A_1(N_{r,x}N_{r,x})+g(N_rN_r)-\omega^2\rho_1A_1(N_rN_r)]dx=\left(\frac{E_1A_1}{L_2}\right)\left[\frac{(1-e^{-j4k_1L_2})}{(1-e^{-j2k_1L_2})^2}\right](jk_1L_2)+g\alpha_1^2\left[-2L_2-j\left(\frac{1}{2k_1}\right)(e^{j2k_1L_2}-e^{-j2k_1L_2})\right]$$

$$K_{rs}=-\int_0^{L_2}[g(N_rN_s)]dx=\begin{cases}g\alpha_1\alpha_3(j)\left[\left(\frac{2k_3}{(k_1^2-k_3^2)}\right)\right][(e^{jk_1L_2}-e^{-jk_1L_2})-(e^{jk_3L_2}-e^{-jk_3L_2})]\\ g(\alpha_\alpha)^2\left[-(e^{jk_\alpha L_2}+e^{-jk_\alpha L_2})L_2-j\left(\frac{1}{k_\alpha}\right)(e^{jk_\alpha L_2}-e^{-jk_\alpha L_2})\right]\end{cases}$$

$$K_{rk}=-\int_0^{L_2}[g(N_rN_k)]dx=\begin{cases}g\alpha_1\alpha_3(j)\left[\left(\frac{1}{k_1+k_3}\right)[e^{j(k_1+k_3)L_2}-e^{-j(k_1+k_3)L_2}]-\left(\frac{1}{k_1-k_3}\right)[e^{j(k_1-k_3)L_2}-e^{-j(k_1-k_3)L_2}]\right], & k_1\neq k_3\\ g(\alpha_\alpha)^2\left[2L_2+j\left(\frac{1}{2k_\alpha}\right)(e^{j2k_\alpha L_2}-e^{-j2k_\alpha L_2})\right], & k_1=k_3=k_\alpha\end{cases}$$

$$K_{sj}=-\int_0^{L_2}[g(N_sN_j)]dx=\begin{cases} g\alpha_1\alpha_3(j)\left[\left(\dfrac{1}{k_1+k_3}\right)(e^{j(k_1+k_3)L_2}-e^{-j(k_1+k_3)L_2})-\left(\dfrac{1}{k_1-k_3}\right)(e^{j(k_1-k_3)L_2}-e^{-j(k_1-k_3)L_2})\right], & k_1\neq k_3\\ g(\alpha_\alpha)^2\left[2L_2+j\left(\dfrac{1}{2k_\alpha}\right)(e^{j2k_\alpha L_2}-e^{-j2k_\alpha L_2})\right], & k_1=k_3=k_\alpha\end{cases}$$

$$K_{sr}=-\int_0^{L_2}[g(N_sN_r)]dx=\begin{cases} g\alpha_1\alpha_3(j)\left[\left(\dfrac{2k_3}{(k_1^2-k_3^2)}\right)\right][(e^{jk_1L_2}-e^{-jk_1L_2})-(e^{jk_3L_2}-e^{-jk_3L_2})], & k_1\neq k_3\\ g(\alpha_\alpha)^2\left[-(e^{jk_\alpha L_2}+e^{-jk_\alpha L_2})L_2-j\left(\dfrac{1}{k_\alpha}\right)(e^{jk_\alpha L_2}-e^{-jk_\alpha L_2})\right], & k_1=k_3=k_\alpha\end{cases}$$

$$K_{ss}=\int_0^{L_2}[E_3A_3(N_{s,x}N_{s,x})+g(N_sN_s)-\omega^2\rho_3A_3(N_sN_s)]dx=\left(\frac{E_3A_3}{L_2}\right)\left[\frac{(1-e^{-j4k_3L_2})}{(1-e^{-j2k_3L_2})^2}\right](jk_3L_2)+g\alpha_3^2\left[-2L_2-j\left(\frac{1}{2k_3}\right)(e^{j2k_3L_2}-e^{-j2k_3L_2})\right]$$

$$K_{sk}=\int_0^{L_2}[E_3A_3(N_{s,x}N_{k,x})+g(N_sN_k)-\omega^2\rho_3A_3(N_sN_k)]dx=-\left(\frac{E_3A_3}{L_2}\right)\left[\frac{2e^{-j3k_3L_2}(-1+e^{j2k_3L_2})}{(1-e^{-j2k_3L_2})^2}\right](jk_3L_2)+g\alpha_3^2\left[(e^{jk_3L_2}+e^{-jk_3L_2})L_2+j\left(\frac{1}{k_3}\right)(e^{jk_3L_2}-e^{-jk_3L_2})\right]$$

$$K_{kj}=-\int_0^{L_2}[g(N_kN_j)]dx=\begin{cases} g\alpha_1\alpha_3(j)\left(\dfrac{2k_1}{(k_1^2-k_3^2)}\right)[(e^{jk_1L_2}-e^{-jk_1L_2})-(e^{jk_3L_2}-e^{-jk_3L_2})], & k_1\neq k_3\\ g(\alpha_\alpha)^2\left[-(e^{jk_\alpha L_2}+e^{-jk_\alpha L_2})L_2-j\left(\dfrac{1}{k_\alpha}\right)(e^{jk_\alpha L_2}-e^{-jk_\alpha L_2})\right], & k_1=k_3=k_\alpha\end{cases}$$

$$K_{kr}=-\int_0^{L_2}[g(N_kN_r)]dx=\begin{cases} g\alpha_1\alpha_3(j)\left[\left(\dfrac{1}{k_1+k_3}\right)[e^{j(k_1+k_3)L_2}-e^{-j(k_1+k_3)L_2}]-\left(\dfrac{1}{k_1-k_3}\right)[e^{j(k_1-k_3)L_2}-e^{-j(k_1-k_3)L_2}]\right], & k_1\neq k_3\\ g(\alpha_\alpha)^2\left[2L_2+j\left(\dfrac{1}{2k_\alpha}\right)(e^{j2k_\alpha L_2}-e^{-j2k_\alpha L_2})\right], & k_1=k_3=k_\alpha\end{cases}$$

$$K_{ks}=\int_0^{L_2}[E_3A_3(N_{k,x}N_{s,x})+g(N_kN_s)-\omega^2\rho_3A_3(N_kN_s)]dx=-\left(\frac{E_3A_3}{L_2}\right)\left[\frac{2e^{-j3k_3L_2}(-1+e^{j2k_3L_2})}{(1-e^{-j2k_3L_2})^2}\right](jk_3L_2)+g\alpha_3^2\left[(e^{jk_3L_2}+e^{-jk_3L_2})L_2+j\left(\frac{1}{k_3}\right)(e^{jk_3L_2}-e^{-jk_3L_2})\right]$$

$$K_{kk}=\int_0^{L_2}[E_3A_3(N_{k,x}N_{k,x})+g(N_kN_k)-\omega^2\rho_3A_3(N_kN_k)]dx=\left(\frac{E_3A_3}{L_2}\right)\left[\frac{(1-e^{-j4k_3L_2})}{(1-e^{-j2k_3L_2})^2}\right](jk_3L_2)+g\alpha_3^2\left[-2L_2-j\left(\frac{1}{2k_3}\right)(e^{j2k_3L_2}-e^{-j2k_3L_2})\right]$$

where

$$\alpha_1=1/(e^{jk_1L_2}-e^{-jk_1L_2}),\quad \alpha_3=1/(e^{jk_3L_2}-e^{-jk_3L_2}),\quad \alpha_\alpha=1/(e^{jk_\alpha L_2}-e^{-jk_\alpha L_2})$$

$$k_1=(\rho_1/E_1)\omega^2,\quad k_3=(\rho_3/E_3)\omega^2,\quad g=(G_2A_2/h_2^2)$$

A.2. Linear shape function

Linear shape function can be Eq. (A.2):

$$N_j=\frac{L_2-x}{L_2},\quad N_{j,x}=-\frac{1}{L_2},\quad N_r=\frac{x}{L_2},\quad N_{r,x}=\frac{1}{L_2}$$

$$N_s=\frac{L_2-x}{L_2},\quad N_{s,x}=-\frac{1}{L_2},\quad N_k=\frac{x}{L_2},\quad N_{k,x}=\frac{1}{L_2}\tag{A.2}$$

Inserting exponential shape function in (A.2) into Eq. (10) yields

$K_{jj}=(1/L_2)(E_1A_1+2pG_2A_2)-(\omega^2/3)(M_1),\quad K_{jr}=(1/L_2)(-E_1A_1+pG_2A_2)-(\omega^2/6)(M_1)$

$K_{js}=-(1/L_2)(2pG_2A_2),\quad K_{jk}=-(1/L_2)(pG_2A_2)$

$K_{rj}=(1/L_2)(-E_1A_1+pG_2A_2)-(\omega^2/6)(M_1),\quad K_{rr}=(1/L_2)(E_1A_1+2pG_2A_2)-(\omega^2/3)(M_1)$

$K_{rs}=-(1/L_2)(pG_2A_2),\quad K_{rk}=-(1/L_2)(2pG_2A_2)$

$K_{sj}=-(1/L_2)(2pG_2A_2),\quad K_{sr}=-(1/L_2)(pG_2A_2)$

$K_{ss}=(1/L_2)(E_3A_3+2pG_2A_2)-(\omega^2/3)(M_3),\quad K_{sk}=(1/L_2)(-E_3A_3+pG_2A_2)-(\omega^2/6)(M_3)$

$K_{kj}=-(1/L_2)(pG_2A_2),\quad K_{kr}=-(1/L_2)(2pG_2A_2)$

$K_{ks}=(1/L_2)(-E_3A_3+pG_2A_2)-(\omega^2/6)(M_3),\quad K_{kk}=(1/L_2)(E_3A_3+2pG_2A_2)-(\omega^2/3)(M_3)$

where,

$$p=\frac{1}{6}\left(\frac{L_2}{h_2}\right)^2,\quad M_1=\rho_1 A_1 L_2=\rho_1(bh_1)L_2,\quad M_3=\rho_3 A_3 L_2=\rho_3(2bh_3)L_2$$

Appendix B. Element of matrix in Eq. (23)

$$k_{11}^i=E_iA_i\int_0^{L_i}\left\{\frac{\partial N_1}{\partial x}\,\frac{\partial N_1}{\partial x}-\omega^2\left(\frac{\rho_i}{E_i}\right)(N_1N_1)\right\}dx=\left(\frac{E_iA_i}{L_i}\right)\left[\frac{(jkL_i)}{(1-e^{-j2kL_i})^2}\right](1-e^{-j4kL_i})$$

$$k_{12}^i=E_iA_i\int_0^{L_i}\left\{\frac{\partial N_1}{\partial x}\,\frac{\partial N_2}{\partial x}-\omega^2\left(\frac{\rho_i}{E_i}\right)(N_1N_2)\right\}dx=\left(\frac{E_iA_i}{L_i}\right)\left[\frac{(jkL_i)}{(1-e^{-j2kL_i})^2}\right][-2e^{-j3kL_i}(-1+e^{j2kL_i})]$$

$$k_{21}^i=E_iA_i\int_0^{L_i}\left\{\frac{\partial N_2}{\partial x}\,\frac{\partial N_1}{\partial x}-\omega^2\left(\frac{\rho_i}{E_i}\right)(N_2N_1)\right\}dx=\left(\frac{E_iA_i}{L_i}\right)\left[\frac{(jkL_i)}{(1-e^{-j2kL_i})^2}\right][-2e^{-j3kL_i}(-1+e^{j2kL_i})]$$

$$k_{22}^i=E_iA_i\int_0^{L_i}\left\{\frac{\partial N_2}{\partial x}\,\frac{\partial N_2}{\partial x}-\omega^2\left(\frac{\rho_i}{E_i}\right)(N_2N_2)\right\}dx=\left(\frac{E_iA_i}{L_i}\right)\left[\frac{(jkL_i)}{(1-e^{-j2kL_i})^2}\right](1-e^{-j4kL_i})$$

or

$$[k_D^i]=\left(\frac{E_iA_i}{L_i}\right)\left[\frac{jkL_i}{(1-e^{-j2kL_i})^2}\right]\left[\begin{array}{c:c}(1-e^{-j4kL_i}) & -2e^{-j3kL_i}(-1+e^{j2kL_i})\\ \hdashline -2e^{-j3kL_i}(-1+e^{j2kL_i}) & (1-e^{-j4kL_i})\end{array}\right]$$

References

[1] A. Baz, Active control of periodic structures, ASME Journal of vibration and Acoustics 123 (2001) 472–479.
[2] D.J. Mead, Free wave propagation in periodically supported, infinite beams, Journal of Sound and Vibration 11 (1970) 181–197.
[3] D.J. Mead, Vibration response and wave propagation in periodic structures, ASME Journal of Engineering for Industry 21 (1971) 783–792.
[4] D.J. Mead, A general theory of harmonic wave propagation in linear periodic systems with multiple coupling, Journal of Sound and Vibration 27 (1973) 235–260.
[5] D.J. Mead, Wave propagation and natueal modes in periodic systems: mono-coupled systems, Journal of Sound and Vibration 40 (1975) 1–18.
[6] D.J. Mead, A new method of analyzing wave propagation in periodic structures; applications to periodic timoshenko beams and stiffened plates, Journal of Sound and Vibration 104 (1986) 9–27.
[7] D.J. Mead, Wave propagation in continuous periodic structures: research contributions from southampton, 1964–1995, Journal of Sound and Vibration 190 (1996) 496–524.
[8] S. Mester, J. Benaroya, Periodic and near periodic structures: review, Shock and Vibration 2 (1995) 69–95.
[9] M. Ruzzene, A. Baz, Active control of wave propagation in periodic fluid-loaded shells, Smart Material and Structure 10 (2001) 893–906.
[10] G. Solaroli, Z. Gu, A. Baz, M. Ruzzene, Wave propagation in periodic stiffened shells: spectral finite element modeling and experiments, Journal of Vibration and Control 9 (2003) 1057–1081.
[11] O. Thorp, M. Ruzzene, A. Baz, Attenuation of wave propagation in fluid-loaded shells with periodic shunted piezoelectric rings, Smart Material and Structure 14 (2005) 594–604.
[12] M. Ruzzene, A. Baz, Control of wave propagation in periodic composite rods using shape memory inserts, Journal of vibration and acoustics, Transactions of ASME 122 (2000) 151–159.
[13] O. Thorp, M. Ruzzene, A. Baz, Attenuation and localization of wave propagation in rods with periodic shunted piezoelectric patches, Smart Material and Structure 10 (2001) 979–989.
[14] M. Toso, A. Baz, Wave propagation in periodic shells with tapered wall thickness and changing material properties, Shock and Vibration 11 (2004) 411–432.
[15] A. Singh, D.J. Pines, A. Baz, Active/passive reduction of vibration of periodic one-dimensional structures using piezoelectric actuators, Smart Material and Structure 13 (2004) 698–711.
[16] D. Richards, D.J. Pines, Passive reduction of gear mesh vibration using a periodic drive shaft, Journal of Sound and Vibration 264 (2003) 317–342.
[17] M. Tawfik, J. Chung, A. Baz, Wave attenuation in periodic helicopter blades, in: Jordan International Mechanical Engineering Conference (JIMEC), Amman, Jordan, 26–28 April 2004.
[18] E.I. Rivin, Passive engine mount-some directions for further development. SAE Paper 850481, 1985.
[19] T. Ushijima, K. Takano, H. Kojoma, High performance hydraulic mount for improving vehicle noise and vibration. SAE Paper 880073, 1988.
[20] R. Singh, G. Kim, R.V. Ravinda, Linear analysis of automotive hydro-mechanical mount with emphasis on decoupler characteristics, Journal of Sound and Vibration 158 (1992) 219–243.
[21] H. Matsuoka, T. Mikasa, H. Nemoto, NV countermeasure technology for a cylinder-on-demand engine-development of active control engine mount, SAE Paper 2004-01-0413, 2004.
[22] L.R. Miller, M. Ahmadian, C.M. Nobles, D.A. Swanson, Modeling and performance of an experimental active vibration isolator, Journal of Vibration and Acoustics 117 (1995) 272–278.
[23] S. Asiri, Vibration attenuation of automotive vehicle engine using periodic mounts, International Journal of Vehicle Noise and Vibration 3 (2007) 302–315.
[24] L. Zheng, W.J. Jung, Z. Gu, A. Baz, Passive periodic engine mount, in: Proceedings of the ASME 2008 International Design Engineering Technical Conferences & Computers and Information in Engineering Conference (IDETC/CIE), New York, NY, USA, August 3–6 2008.